NATIONAL ADVISORY COMMITTEE FOR AERONAUTICS

TECHNICAL NOTE

No. 1748

CALCULATION OF TUNNEL-INDUCED UPWASH VELOCITIES FOR SWEPT AND YAWED WINGS

By S. Katzoff and Margery E. Hannah

Langley Aeronautical Laboratory
Langley Field, Va.

Washington
November 1948

NATIONAL ADVISORY COMMITTEE FOR AERONAUTICS

TECHNICAL NOTE NO. 1748

CALCULATION OF TUNNEL-INDUCED UPWASH VELOCITIES FOR SWEPT AND YAWED WINGS

By S. Katzoff and Margery E. Hannah

SUMMARY

The tunnel-induced upwash field for a point element of lift in a rectangular tunnel is shown to consist of three superimposed fields that, except for relative position, are independent of the lateral or longitudinal location of the lift element in the tunnel. One of these fields is also independent of the type of tunnel (open or closed) and of the width-height ratio of the tunnel, and the other two, which depend on this ratio, are identical (except, perhaps, for sign). A contour chart of the first field is given in the present paper; hence, only one other contour chart need be calculated for any given tunnel to permit the determination of the induced upwash field for any position of the lifting element. Contour charts of this other field are given for three specific tunnels: an open tunnel of 2:1 width-height ratio, a closed tunnel of 2:5 width-height ratio, and a closed tunnel of 10:7 width-height ratio. By superposition of results for various locations of the lifting element, the total field may be found for a wing of any plan form and with any distribution of lift.

For tunnels that are not rectangular or that cannot be considered approximately rectangular, the corresponding procedure requires the preparation of a chart for each of several spanwise locations of the lifting element. Even this procedure appears simpler and more generally applicable than the calculation of induced upwash for a series of wing spans and sweep angles.

INTRODUCTION

As is well known, the calculation of subsonic wind-tunnel-wall interference at a straight unyawed lifting line is reducible to a relatively simple two-dimensional flow problem; whereas the corresponding calculation for a yawed or swept lifting line or the calculation of induced camber or of the downwash correction at the tail cannot be similarly simplified. Because of the present intensive study of swept-wing and triangular-wing configurations, much effort is being directed toward evaluation of tunnel interference for such wings. In general the calculations are very cumbersome (see, for example, references 1 and 2), not only because of the three-dimensional character of the flow

problem but also because the preparation of a comprehensive set of corrections for a particular wind tunnel entails calculations for at least a two-parameter family of wings, that is, for wings of various spans and various sweep angles.

In some recent studies made at the Langley Laboratory it became evident that making computations of tunnel-interference flows for a two-parameter family of wings was an unnecessary complication. Results of equal accuracy can be achieved by a somewhat different and much more flexible method which, in general, requires computation of only a one-parameter family of charts and, for a rectangular tunnel, requires the computation of only two charts. Furthermore, the computations for these charts, which can be used for any wing, are generally simpler than the computation of the tunnel interference field for a particular wing by the usual method (in which the wing loading is represented by a combination of yawed horseshoe vortices).

The proposed procedure is possibly known at some aeronautical laboratories. Because of its apparent absence from the literature, however, and because procedures similar to those of references 1 and 2 appear to be in general use, the present paper has been prepared which outlines the method, describes the computations, and gives examples of the derived charts. This paper is concerned exclusively with the calculation of tunnel-induced vertical velocities in the horizontal center plane of the tunnel, corresponding to a specified load distribution on the wing, which is also assumed to lie in the same plane. Modification of the procedure would be required for application to triangular or highly swept wings at very high angles of attack. No effort is made to discuss the corrections to the measured force and moment characteristics, since the effects of the induced upwash velocity on these characteristics are discussed in reference 1.

SYMBOLS

Γ	strength of horseshoe vortex
Δs	span of horseshoe vortex
ΔL	lift of wing segment
ΔS	area of wing segment
c_l	mean lift coefficient of wing segment
C_L	wing lift coefficient
S	wing area

ρ	air density
V	stream velocity
b	tunnel width
h	tunnel height
x	longitudinal coordinate
y	lateral coordinate
z	vertical coordinate
w	upwash velocity
C	tunnel cross-sectional area
D	cross-sectional area of tunnel having same proportions as actual tunnel, but in which tunnel width is unity
+	semi-infinite doublet line, similar to doublet line in tunnel
−	semi-infinite doublet line, reverse of doublet line in tunnel
$\hat{\sigma}$	semi-infinite source line
$\hat{\rho}$	semi-infinite sink line
a, b, c, and d	points on wing where lift is assumed to be concentrated
a', b', c', and d'	nearest lateral images of points a, b, c, and d
α, β, and γ	points on wing where tunnel-induced upwash angles are to be determined

CALCULATION OF TUNNEL INTERFERENCE

Representation of Wing Loading

For purposes of computing the tunnel interference by the method to be described, the assumed loading on the wing is approximated by a distribution of point concentrations of lift, about as indicated in figure 1. Roughly, this distribution is chosen by considering the

wing area to be made up of several smaller areas or segments, estimating the lift on each, and locating each equivalent point concentration of lift at the approximate centroid of the lift on each segment. As has frequently been shown, the tunnel interference field is determined mainly by the total lift and the total rolling moment and is otherwise relatively independent of the precise lift distribution (references 3 and 4); accordingly, representing the continuous loading by several discrete point concentrations in the indicated manner is normally satisfactory for the calculation of the tunnel interference field. In any event, where a question arises as to the adequacy of the representation used (as in the case of large-span wings), accuracy can be improved by increasing the number of points or even extending the procedure from a summation to a graphical or numerical integration.

Associated with each concentration of lift is a horseshoe vortex of infinite strength and zero span extending downstream from the point where the lift is considered to be concentrated. The moment $\Gamma\Delta s$ of each horseshoe vortex is given by the lift equation $\Delta L = \rho V \Gamma \Delta s$. Since the field of such a degenerate horseshoe vortex is easily shown to be equivalent to that of a line of source-sink doublets (reference 5), it will be referred to, for convenience, as a doublet line. The problem to be discussed in the succeeding sections, then, is the determination of the tunnel-interference flow resulting from the presence of a group of doublet lines similar to that indicated in figure 1.

Rectangular Tunnels

Image system and interference field for closed tunnel.- Figure 2(a) shows the image system for one doublet line located in the horizontal plane of symmetry of a closed rectangular tunnel. The tunnel boundary is indicated by heavy lines and the boundaries of the image tunnels are indicated by light lines. The image doublets are represented by plus or minus signs according as they are the same as, or the reverse of, the doublet in the tunnel. This image system satisfies the boundary condition that the velocity components normal to the walls must be zero.

The complete system of doublets in figure 2(a) is seen to comprise two superimposed, doubly infinite, 2b by h rectangular arrays of doublets. One array, indicated by circles, may be considered as centered at the original doublet (double circle) in the tunnel; the other array, indicated by squares, may be considered as centered at the nearest horizontal image doublet (double square).

The interference field is thus made up of two parts:

(a) The field of a complete rectangular array having its center at the double square.

(b) The field of a complete rectangular array having its center at the double circle with, however, the field of the center doublet omitted (since it represents the lifting element itself).

Basis of proposed calculation procedure.— The dimensions of each array, and hence its associated flow field, are determined only by the dimensions of the tunnel and are independent of the lateral or longitudinal location of the lifting element in the tunnel. Accordingly, once the two fields have been calculated, they may be used for finding the interference corresponding to a lifting element located anywhere in the horizontal center plane of the given closed rectangular tunnel. The procedure is indicated in figure 3 which shows (plan view) a lifting element and its nearest image. In figure 3(a) is indicated the contour chart of induced upwash velocities calculated for a 2b by h doubly infinite array of unit doublets with the center doublet omitted. The point on the contour chart that is located at the head of the omitted doublet line is indicated as the origin; and the chart is placed so that this point falls on the lifting element, designated a. In figure 3(b) is indicated the contour chart for the complete doubly infinite array, placed so that its origin falls on the first image, designated a'. At any specified point α in the horizontal center plane of the tunnel, the induced upwash corresponding to the given element of lift is found by adding the values read at that point from the contour charts in figures 3(a) and 3(b) and multiplying the sum by the strength of the equivalent doublet.

The procedure may be slightly modified to take advantage of the fact that the chart of figure 3(b) is equivalent to the sum of two other charts, namely, the chart of figure 3(a), which is for the doubly infinite array with the center doublet omitted, and a chart for a single doublet (that which is omitted in the chart of figure 3(a)). Accordingly, the chart of figure 3(a) and a chart for a single doublet should suffice to obtain the desired upwash values. In this modification, the step indicated in figure 3(b) is replaced by the two steps indicated in figures 4(a) and 4(b). Three readings are thus necessary instead of two; since the chart for a single doublet is given in the present paper (fig. 5), however, this modification requires that only the chart of figure 3(a) be prepared for each given rectangular tunnel.

Image systems for other rectangular tunnels.— In figures 2(b) to 2(f), are shown the image systems for five other rectangular tunnels, namely, those that are, respectively,

(1) Open on all four sides

(2) Closed at the sides but open at the top and bottom

(3) Closed at the top and bottom but open at the sides

(4) Closed only at the bottom

(5) Closed, containing a semispan reflection model

Open boundaries are indicated by dashed lines and closed boundaries, by solid lines. In each of these cases, as with the completely closed tunnel, the image system is seen to be composed of two 2b by h rectangular arrays so that the procedure just outlined should also apply for these configurations, except that for some of the tunnels, however, the two arrays have opposite signs so that the readings from figures 4(a) and 4(b) must be subtracted from, instead of added to, those from figure 3(a). The rectangular arrays are not, however, all of the same type as for the completely closed tunnel. The image systems can be briefly described as follows:

For a closed tunnel (fig. 2(a)), each array consists of alternate horizontal rows of plus and minus doublets, and the two arrays have the same sign (that is, the nearest horizontal image is plus).

For an open tunnel (fig. 2(b)), all the doublets of each array have the same sign, but the two arrays have opposite signs.

For a tunnel closed at the sides but open at the top and bottom (fig. 2(c)), all the doublets of each array have the same sign and the two arrays also have the same sign; that is, only plus doublets occur in the image system.

For a tunnel closed at the top and bottom but open at the sides (fig. 2(d)), each array consists of alternate rows of plus and minus doublets, and the two arrays have opposite signs.

For a tunnel closed only at the bottom (fig. 2(e)), the signs for the image system in the first, third, fifth, . . . rows above the plane of the wing are, respectively, opposite to those in the first, third, fifth, . . . rows below the plane of the wing. Since the net effect of the odd numbered rows on the upwash velocity in the center plane is thus zero, they may be neglected. Two 2b by 2h arrays remain having alternate rows of plus and minus doublets and the two arrays have opposite signs.

For a closed tunnel containing a semispan reflection model (fig. 2(f)), each array has alternate rows of plus and minus doublets and the two arrays have the same sign. In the indicated image system the image in the double square, which represents the second half of the reflection model, must, like the model itself, be excluded from consideration in calculating the interference field. The reflection system thus consists of two arrays in each of which the central doublet is omitted. For this case, then, only one chart (similar to that of fig. 3(a)) is used. The same conclusion applies whenever a semispan reflection model is tested with a tunnel wall as the reflection plane. As a corollary, it follows that, if a tunnel is used to test only symmetrical, unyawed, full-span models, only one contour chart need be prepared, and the chart would represent the field of a b by h (instead of a 2b by h) array. This conclusion can be readily verified by examining figure 2(g) which represents a closed tunnel containing a

full-span symmetrical model and which is identical with figure 2(f) except that the reflection plane and all its images are omitted.

Basic formulas and summation procedures for calculating contour charts.- The potential of a unit doublet at the origin with its axis vertical is

$$\frac{z}{4\pi\left(x^2 + y^2 + z^2\right)^{3/2}}$$

The potential of a doublet line extending along the x-axis from the origin to infinity is then

$$\Phi = \frac{1}{4\pi}\int_0^\infty \frac{z\,dx'}{\left[(x - x')^2 + y^2 + z^2\right]^{3/2}}$$

$$= \frac{1}{4\pi}\frac{z}{y^2 + z^2}\left(1 + \frac{x}{\sqrt{x^2 + y^2 + z^2}}\right)$$

The corresponding upwash velocity is

$$w = \frac{\partial\Phi}{\partial z} = \frac{1}{4\pi}\left\{\frac{y^2 - z^2}{\left(y^2 + z^2\right)^2} + \frac{x\left[\left(y^2 + z^2\right)\left(x^2 + y^2 - 2z^2\right) - 2x^2z^2\right]}{\left(y^2 + z^2\right)^2\left(x^2 + y^2 + z^2\right)^{3/2}}\right\} \qquad (1)$$

For any particular array of unit doublets, the upwash velocity at a point (the contour value at that point on the contour chart) is the sum of the values given by this formula for a series of values of y differing by $2b$ and a series of values of z differing by h, with appropriate signs according to the type of array. Such a double series usually converges rather slowly, however, and, in general, the practicability of the summation depends on the use of certain approximation methods for summing the fields of all but an inner group of doublets surrounding the origin. These approximation methods, which are very similar to those used in the two-dimensional studies of reference 6, are reviewed in the following paragraphs.

The field of a doublet line is approximately the same as the field of a horseshoe vortex of the same moment, provided the distance from the doublet line to the point where the field is being considered is sufficiently large relative to the span of the horseshoe vortex. Thus, in computing the field near $y = 0$, a row of equal doublets at, for instance, $y = 4b$, $6b$, $8b$, . . . may be replaced by a row of horseshoe vortices of span $2b$ having their trailing vortices at $y = 3b$ and $5b$, $5b$ and $7b$, $7b$ and $9b$, . . . In this representation, all the trailing vortices except the innermost one cancel in pairs, so that the infinite row of doublets is

equivalent to an L-vortex of which the trailing portion is at $y = 3b$ and of which the bound portion extends along the y-axis from $3b$ to infinity. The field of this infinite L-vortex is easily calculated by the Biot-Savart law.

For a horizontal row of doublets lying a reasonable distance above the origin, all may be replaced by horseshoe vortices of span $2b$, in which case all the trailing vortices cancel in pairs and only the bound vortex extending from $-\infty$ to $+\infty$ remains. Its field is merely that of a two-dimensional vortex.

By means of the approximate representations just described, a rectangular array of doublets in which the alternate rows have plus and minus signs can be assumed approximately equivalent to an inner group of doublets around the origin (those that are too close to be adequately replaced by horseshoe vortices) and an outer arrangement of L-vortices and two-dimensional bound vortices (fig. 6(a)). Because of the alternating signs, the upwash velocity at any point due to the two-dimensional bound vortices may be formulated as the sum of the terms of an alternating series, which can be readily evaluated.

For a rectangular array of doublets in which all have the same sign, a different replacement system is more convenient. Instead of being extended horizontally into a horseshoe vortex, the doublet is extended vertically into a source line and a sink line, a distance h apart. The source lines and sink lines in any column cancel each other in pairs and only the source or sink lines, at a distance $\frac{h}{2}$ above or below the inner group of doublets, remain. This equivalent representation for a rectangular array in which all doublets have the same sign is shown in figure 6(b).

It may be noted that the previously mentioned L-vortices are actually horseshoe vortices of which the second trailing vortex is at $y = \infty$ and that similar trailing vortices at $y = \pm\infty$ are associated with the infinite bound vortices. Similarly, where the source lines and sink lines in the columns cancel each other in pairs, a row of sink lines remain at $z = +\infty$ and a row of source lines at $z = -\infty$. The trailing vortices at $y = \pm\infty$ require no special consideration because their alternating signs would, in any event, result in zero net effect in the region of the origin. The sink and source lines, however, would be expected to result in a uniform upwash throughout the field, provided the extent of the rows of source and sink lines is of a higher order of infinity than is their distance from the origin. For the open tunnel (fig. 2(b)), whether this uniform vertical velocity is included or not is immaterial, since the two arrays have opposite signs and the uniform upwash would thereby be eliminated in any case. The question still remains, however, for the tunnel of figure 2(c), where the two arrays have the same sign. Actually, a discussion of the relative orders of the two infinities is not necessary or desirable inasmuch as a simple physical criterion is available for such cases, namely, that the total induced upwash should approach zero at a large distance upstream from the wing. Since the field indicated

in figure 6(b) already satisfies this upstream boundary condition, the uniform upwash that would result from the source and sink lines at infinity should clearly not be included.

Remarks on preparation of charts and scale factors.— In the calculations for the charts, it is convenient to consider the tunnel width as unity and to assume unit doublets in the array (that is, to use equation (1) for the field of each doublet). The half-width of the charts need never exceed 1.5 tunnel widths, as is obvious from figure 4. An example of a complete chart, used in estimating corrections for the Langley full-scale tunnel (idealized to a 60- by 30-foot rectangular tunnel), is shown in figure 7(a). The tunnel was considered as a 1 unit by 1/2 unit rectangle, so that the tunnel area D was 1/2 and the doublet images formed a 2 by 1/2 array. The chart half-width is considerably less than 1.5 tunnel widths because results for this case showed that the outer contour values, when added to those of figure 5, were insignificant. In figure 7(b) is shown a chart for a closed 3- by 7.5-foot rectangular tunnel. The chart was computed for a 2 by 2.5 array of unit doublets corresponding to a tunnel area D of 2.5. Figure 7(c) shows a chart similarly developed for 7- by 10-foot rectangular tunnels.

The chart of figure 5 for the single unit doublet, as computed from equation (1) with $z = 0$, was plotted with the unit distance indicated on the coordinate axes. In keeping with the preceding discussion, the chart half-width is 1.5 units.

The scale factor for the eventual application of the charts is developed as follows:

The lift ΔL associated with a horseshoe vortex of strength Γ and span Δs (actual wing dimensions) is given by

$$\Delta L = c_l \Delta S \frac{\rho V^2}{2}$$

$$= (\Gamma \Delta s) \rho V$$

from which

$$\Gamma \Delta s = \frac{c_l \Delta S V}{2}$$

which is the equivalent doublet strength of a segment of wing area ΔS having a mean lift coefficient c_l. The chart contours give the upwash velocity w for a doublet of unit strength in a tunnel of cross-sectional area D. For the case of a doublet of strength $\Gamma \Delta s$ in a tunnel of area C,

$$w = \text{Chart reading} \times \Gamma \Delta s \times \frac{D}{C}$$

or, with $\Gamma\Delta s$ replaced by $c_l\Delta SV/2$, the upwash angle in radians is

$$\frac{w}{V} = \text{Chart reading} \times \frac{c_l\Delta SD}{2C}$$

or in degrees,

$$\text{Chart reading} \times \frac{28.6c_l\Delta SD}{C}$$

If the suggested convention — that the tunnel width be taken as unity in computing the charts — is followed, then the factor D/C is merely $1/b^2$ and the expression for the upwash angle in degrees is

$$\text{Chart reading} \times \frac{28.6c_l\Delta S}{b^2}$$

Use of charts in computation of tunnel interference flow.— Assume that corrections are desired for a closed rectangular tunnel, for which a chart of the type shown in figure 7 (that is, for an infinite array of doublets with the center doublet omitted) has been prepared. This chart is designated chart A. The chart of figure 5, for a single doublet, is designated chart B. The procedure may then be outlined as follows:

(1) Sketch the complete wing to the scale of the charts. Show the sides of the tunnel and the nearest images of the semispans (fig. 8).

(2) Assume the lift to be concentrated at, say, two points on each semispan, and estimate the lift at each point in terms of $c_l\Delta S$. The sum of the four values of $c_l\Delta S$ must equal $C_L S$ for the complete wing. Also, if rolling moments are being considered, the rolling-moment coefficient of the approximate representation should equal the rolling-moment coefficient of the wing. Indicate on the sketch the four points a, b, c, and d and their nearest images a', b', c', and d'. Also, locate on the sketch the points at which the tunnel-induced angle is desired, say α, β, and γ. In general, where only a few points are used, greatest accuracy is achieved by assuming the lift (in the case of an unflapped wing) to be concentrated along the $\frac{1}{4}$-chord line and determining the upwash angles along the $\frac{3}{4}$-chord line, as indicated in figure 8. (The drag correction, however, is probably more correctly determined from the upwash angles at the $\frac{1}{4}$-chord line where the lift is concentrated.)

(3) Place the origin of chart A at point a and read the chart contours at α, β, and γ. Repeat for points b, c, and d. Then place

the origin of chart A at point a' and read the chart contours at α, β, and γ. Repeat for points b', c', and d'. Finally, place the origin of chart B at point a' and read the chart at α, β, and γ. Repeat for points b', c', and d'.

(4) Finally, for the upwash angle at, say, point α, find the algebraic sum of the three chart readings (for example, (a,α) and (a',α) from chart A and (a',α) from chart B) for each of the four points a, b, c, and d. Multiply each of these four sums by the value of $\frac{28.6}{b^2}c_l\Delta S$ for the wing segment under consideration (a, b, c, or d) and add. The total is the tunnel-induced upwash angle, in degrees, at point α. Proceed similarly for points β and γ.

When the vertical symmetry plane of the tunnel is also the vertical symmetry plane of the wing (in general, for zero yaw and zero aileron deflection), the work can be somewhat reduced. Only two load points a and b on the wing and their two reflections a' and b' need be used, although the chart readings must still be obtained at the two symmetrically located points α and γ on both sides of the wing. The net induced angle at α or γ is obtained by adding the results for α and γ; the net induced angle at β is obtained by doubling the result for β.

Nonrectangular Tunnels

For a circular or other nonrectangular tunnel, the problem cannot be reduced to that of calculating a single chart. A series of contour charts, giving the tunnel-induced upwash in the horizontal center plane of the tunnel, must be constructed for a series of spanwise locations of the doublet in the tunnel. Even so, only a single parameter — the spanwise location of the doublet — is involved, since variations in longitudinal location of the lifting element (such as those for the different lifting elements along a swept wing) are readily taken into account by longitudinal shift of the contour chart. From a study of reference 2 it appears reasonably certain not only that the calculations herein proposed would have been easier than the calculations therein indicated but also that the eventual application of the results to wings of irregular load distributions would also have been easier. The procedure indicated in reference 7 seems to be of this type.

With regard to studies similar to those of reference 2, it may be of value to point out that, at least theoretically, a series of calculations for any one sweep angle should suffice for computing the tunnel effect for any other sweep angle. Figure 9(a) shows, for example, how the loading on a 60° swept wing may be approximated by a single horseshoe vortex and two pairs of unswept horseshoe vortices, where the inner vortex of each pair has the same strength as the superimposed outer vortex but has opposite rotation. Figure 9(b) shows, similarly, how a pair of horseshoe vortices and a single horseshoe vortex, all

swept 45°, might be used to approximate the loading on a 60° swept wing with sufficient accuracy to calculate the tunnel interference velocities.

CONCLUDING REMARKS

For a lifting wing of arbitrary loading and plan-form, situated in the horizontal center plane of a rectangular tunnel, the tunnel-induced upwash velocities in the same plane can be readily calculated with the aid of two charts. One is given in the present paper; the other must be computed for each tunnel. Such simplification is not possible for nonrectangular tunnels. In any case, however, computations for a series of wings of various spans and various sweep angles are unnecessary. Thus, computations for several spanwise positions of the lifting element or computations for a set of unswept wings of various spans should provide a basis for computing tunnel-induced upwash velocities for any wing in the horizontal center plane of the tunnel.

Langley Aeronautical Laboratory
National Advisory Committee for Aeronautics
Langley Field, Va., July 27, 1948

REFERENCES

1. Swanson, Robert S.: Jet-Boundary Corrections to a Yawed Model in a Closed Rectangular Wind Tunnel. NACA ARR, Feb. 1943.

2. Eisenstadt, Bertram J.: Boundary-Induced Upwash for Yawed and Swept-Back Wings in Closed Circular Wind Tunnels. NACA TN No. 1265, 1947.

3. Glauert, H.: Wind Tunnel Interference on Wings, Bodies and Airscrews. R. & M. No. 1566, British A.R.C., 1933.

4. Koning, C., and van der Maas, H. J.: Onderzoek van de werking van stuurklappen aan een dikken tapschen vleugel. Rep. No. A 32, Verslagen en Verhandelingen R.S.L. (Amsterdam), Deel IV, 1927, appendix III, pp. 240–255.

5. Joos, Georg: Theoretical Physics. Blackie and Son Ltd. (London), 1934, p. 292.

6. Theodorsen, Theodore: The Theory of Wind-Tunnel Wall Interference. NACA Rep. No. 410, 1931.

7. Von Kármán, Th., and Burgers, J. M.: General Aerodynamic Theory – Perfect Fluids. Influence of Boundaries in the Field of Motion around Airfoil Systems. Vol. II of Aerodynamic Theory, div. E, ch. IV, pt. C, W. F. Durand, ed., Julius Springer (Berlin), 1935, pp. 265–273.

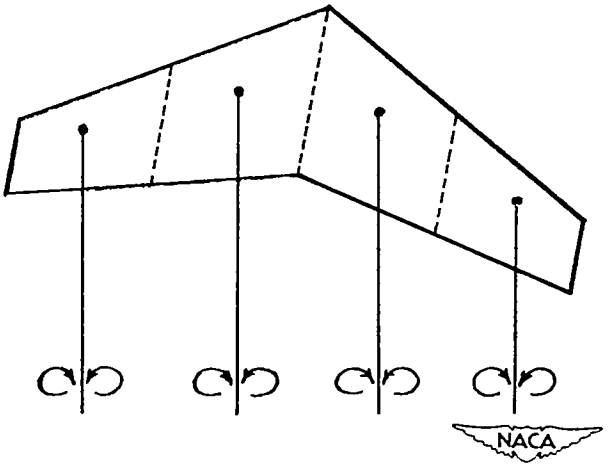

Figure 1.- Field of a lifting wing represented as the field of four doublet lines extending downstream from four points where the lift is assumed to be concentrated.

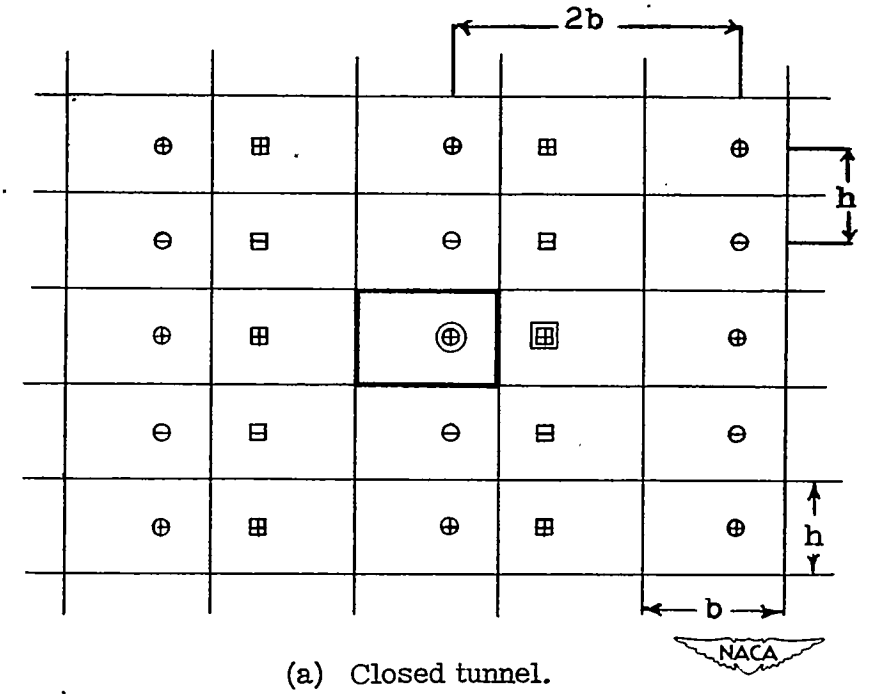

(a) Closed tunnel.

Figure 2.- Image configurations for doublet lines in rectangular tunnels. Doublet in tunnel is indicated by double circle; nearest lateral image is indicated by double square.

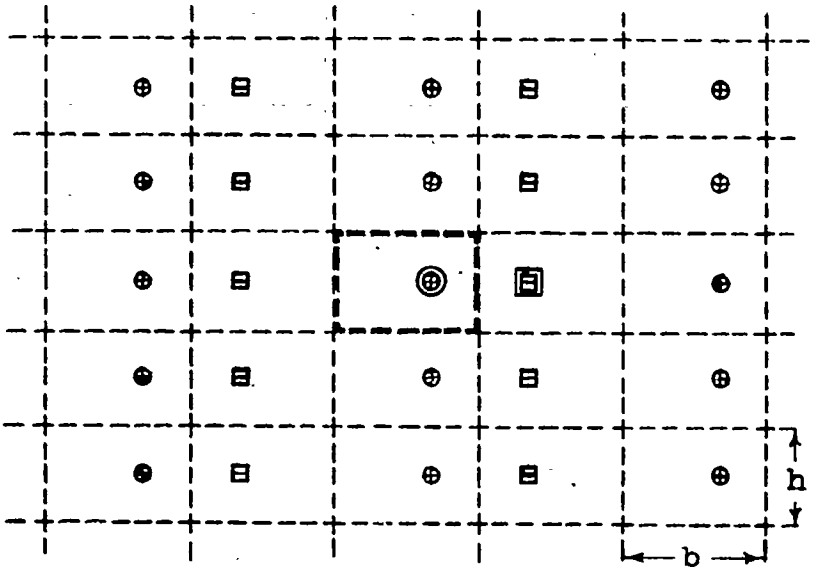

(b) Open tunnel.

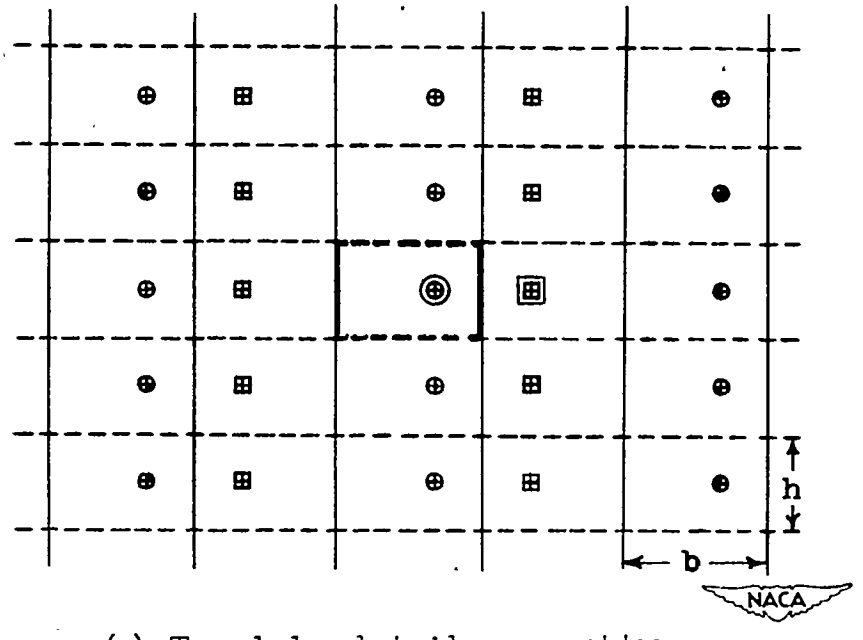

(c) Tunnel closed at sides, open at top and bottom.

Figure 2.- Continued.

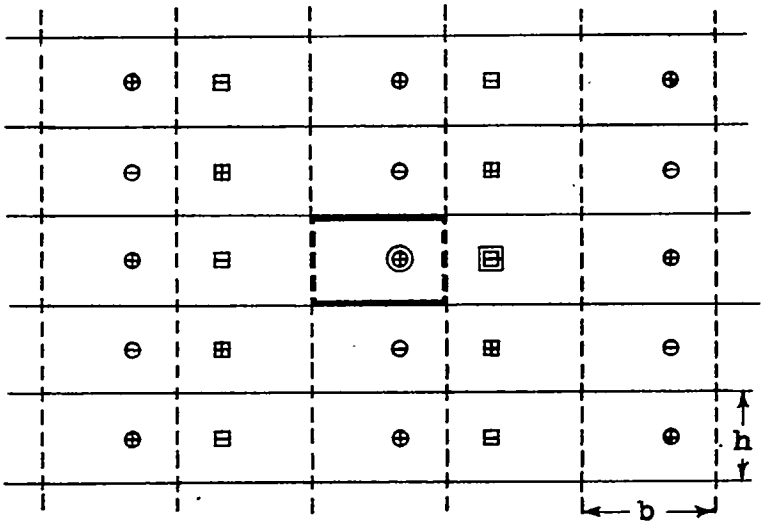

(d) Tunnel closed at top and bottom, open at sides.

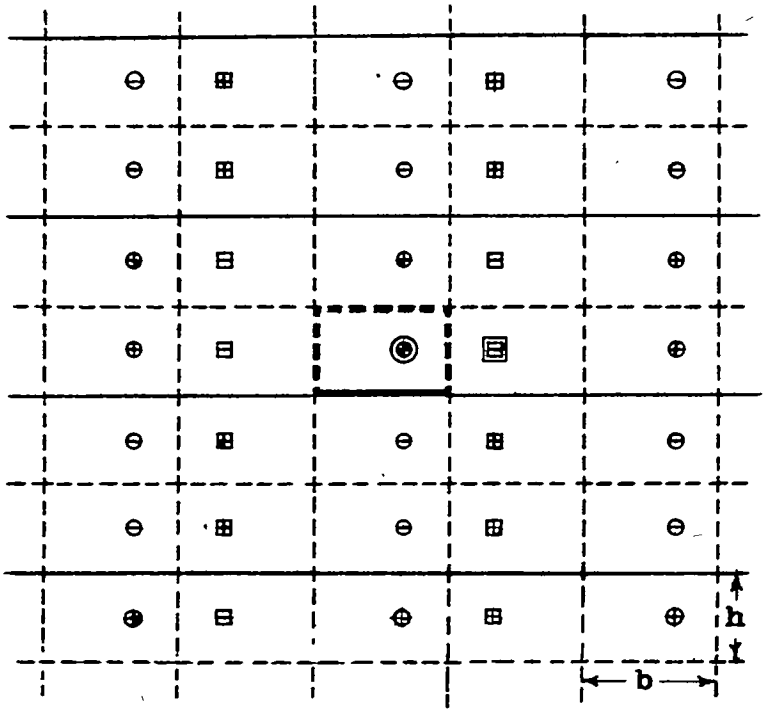

(e) Tunnel closed at bottom, open on three sides.

Figure 2.- Continued.

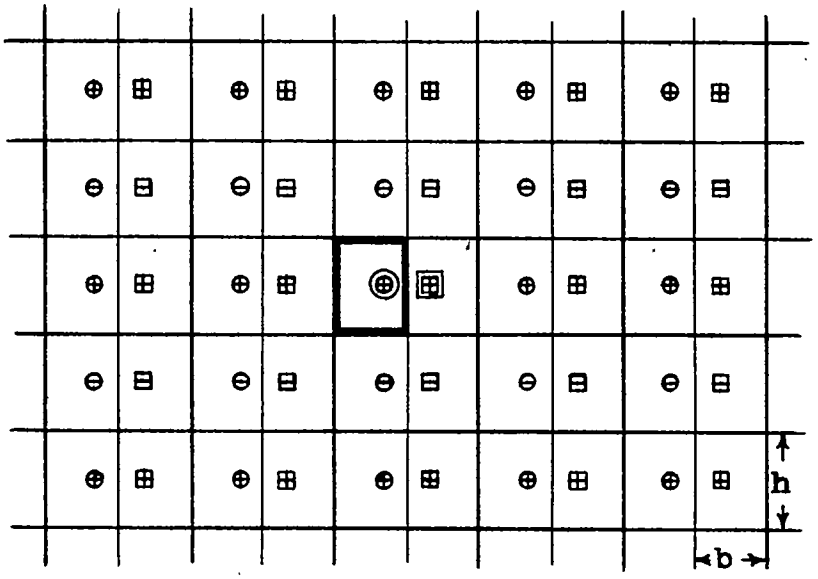

(f) Closed tunnel containing a semispan reflection model.

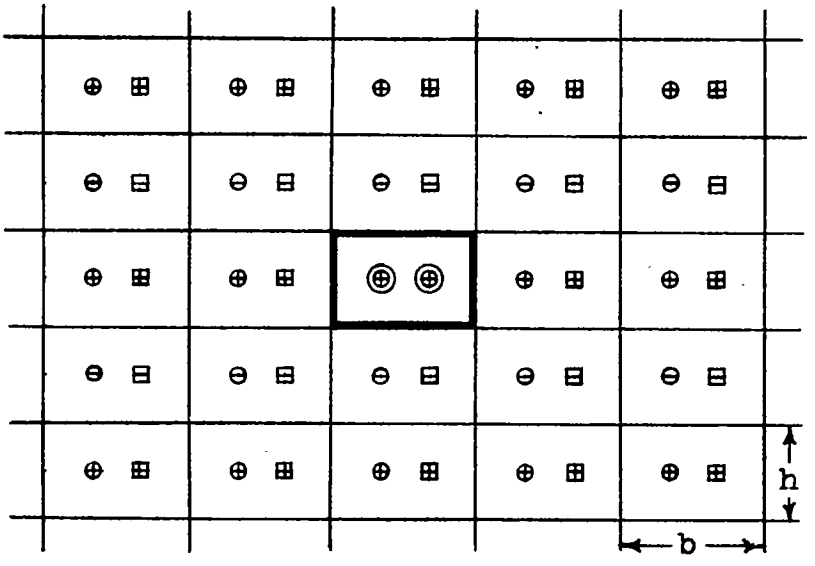

(g) Closed tunnel containing a full-span symmetrical model.

Figure 2.- Concluded.

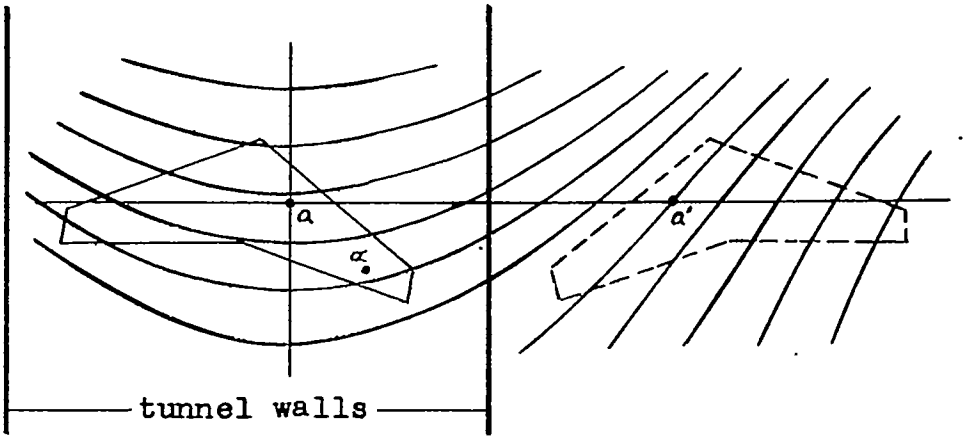

(a) Chart representing field of doubly infinite array of unit doublets with center doublet omitted; origin of chart is placed on point a.

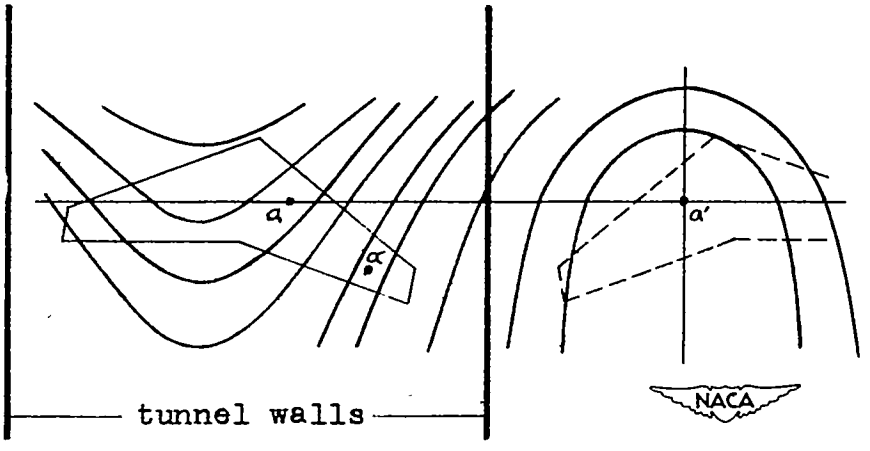

(b) Chart representing field of complete doubly infinite array of unit doublets; origin of chart is placed on nearest image a'.

Figure 3.- Tunnel interference velocity at point α, corresponding to lift concentration at point a, determined by two contour charts.

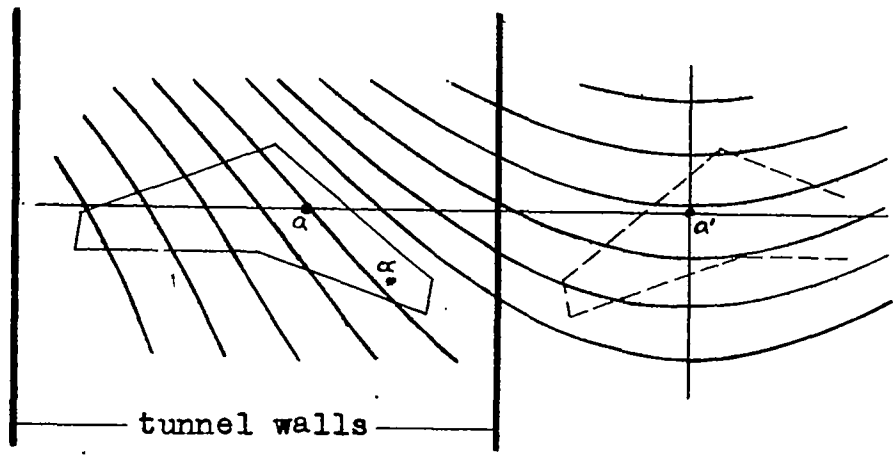

(a) Same as the chart of figure 3(a); origin at a'.

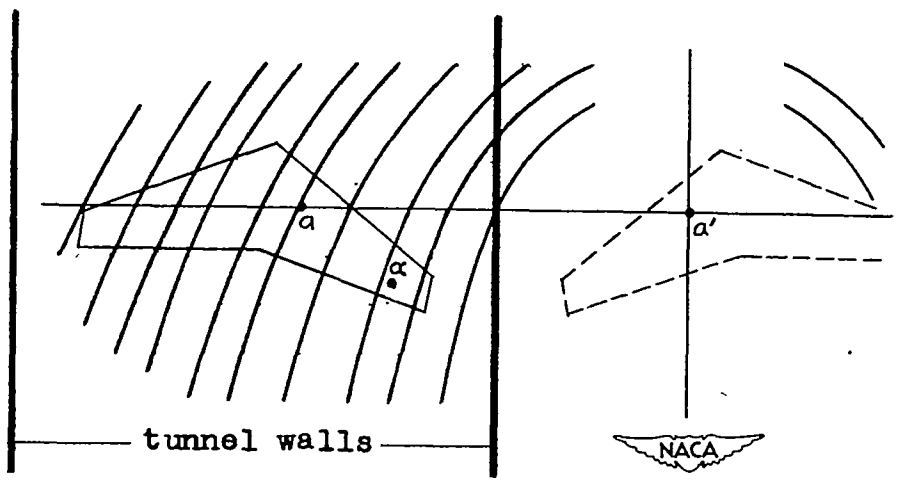

(b) Chart representing field of a single unit doublet.

Figure 4.- Two contour charts, the sum of which equals the chart of figure 3(b).

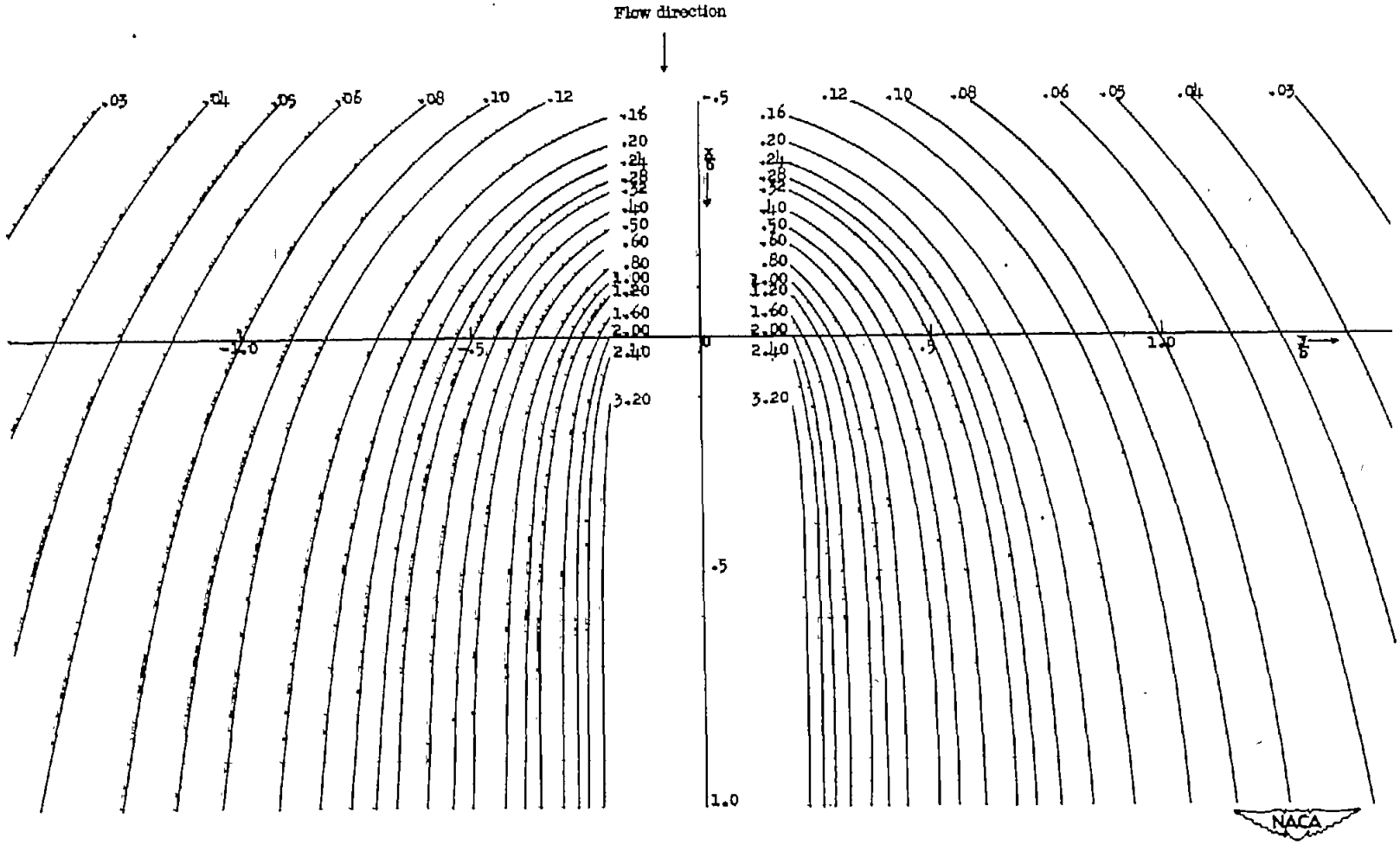

Figure 5.- Chart B. Contours of upwash velocity due to a unit positive semi-infinite doublet line. The origin 0 is the head of the doublet line.

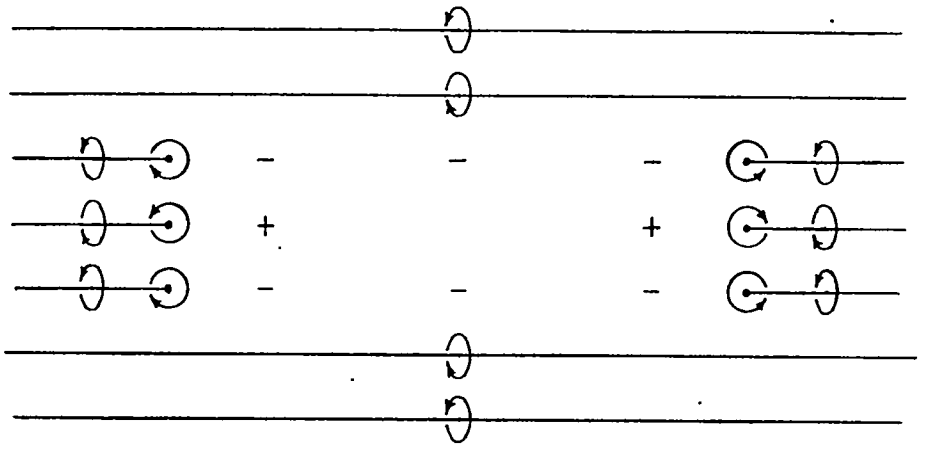

(a) Array having alternate rows of plus and minus doublets.

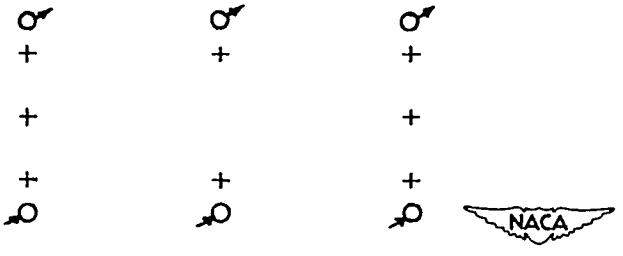

(b) Array having only plus doublets.

Figure 6.- Approximate representations of the two types of doubly infinite, rectangular arrays of doublets with center doublet omitted.

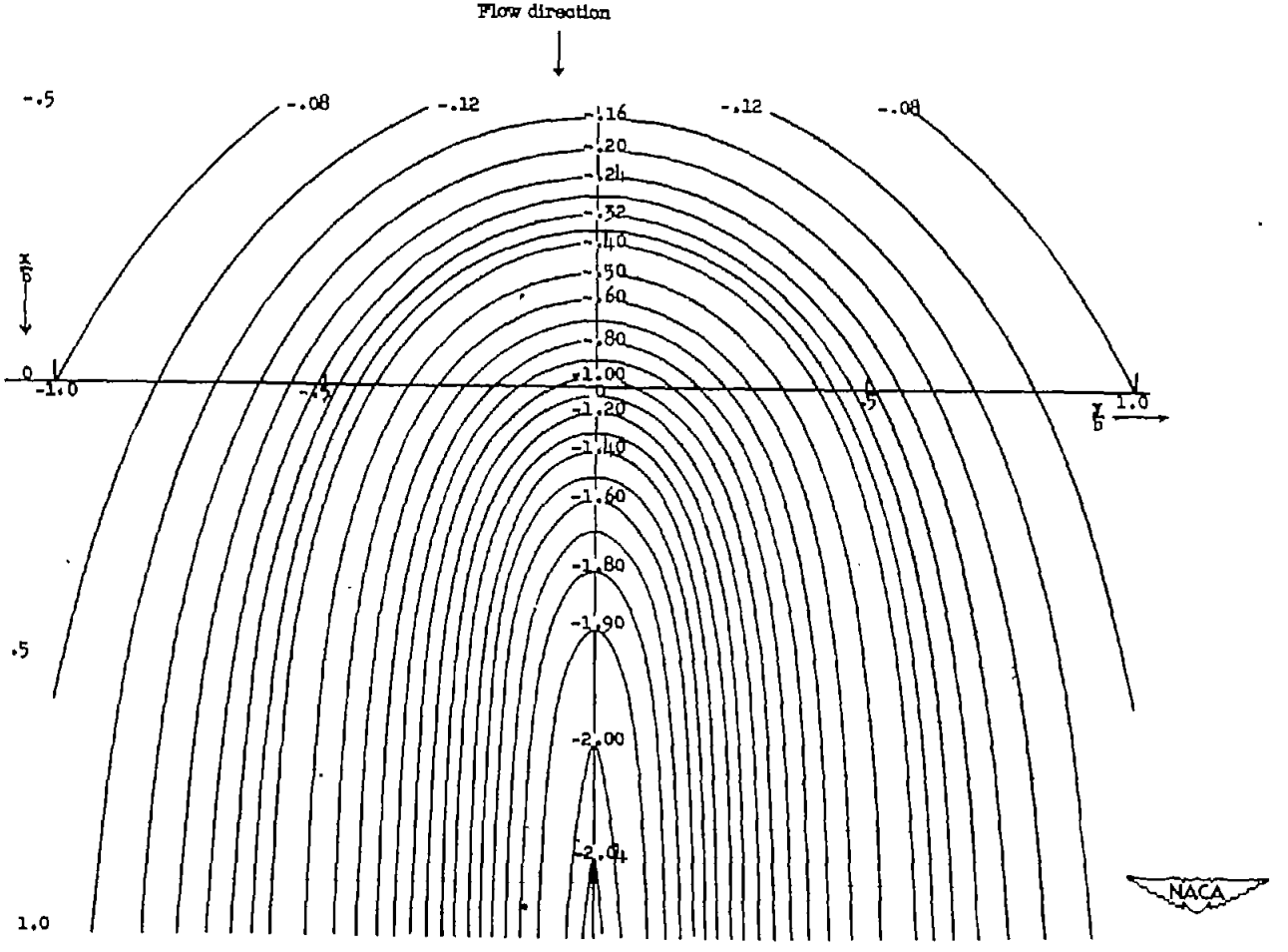

(a) Chart used in deriving corrections for the Langley full-scale tunnel; calculated for a 2 (horizontal) by 0.5 (vertical) array, with all doublets positive.

Figure 7.- Examples of chart A. Contours of upwash velocity in the horizontal center plane due to a doubly infinite array of unit semi-infinite doublet lines with the center doublet line omitted. The origin 0 is the head of the center doublet line.

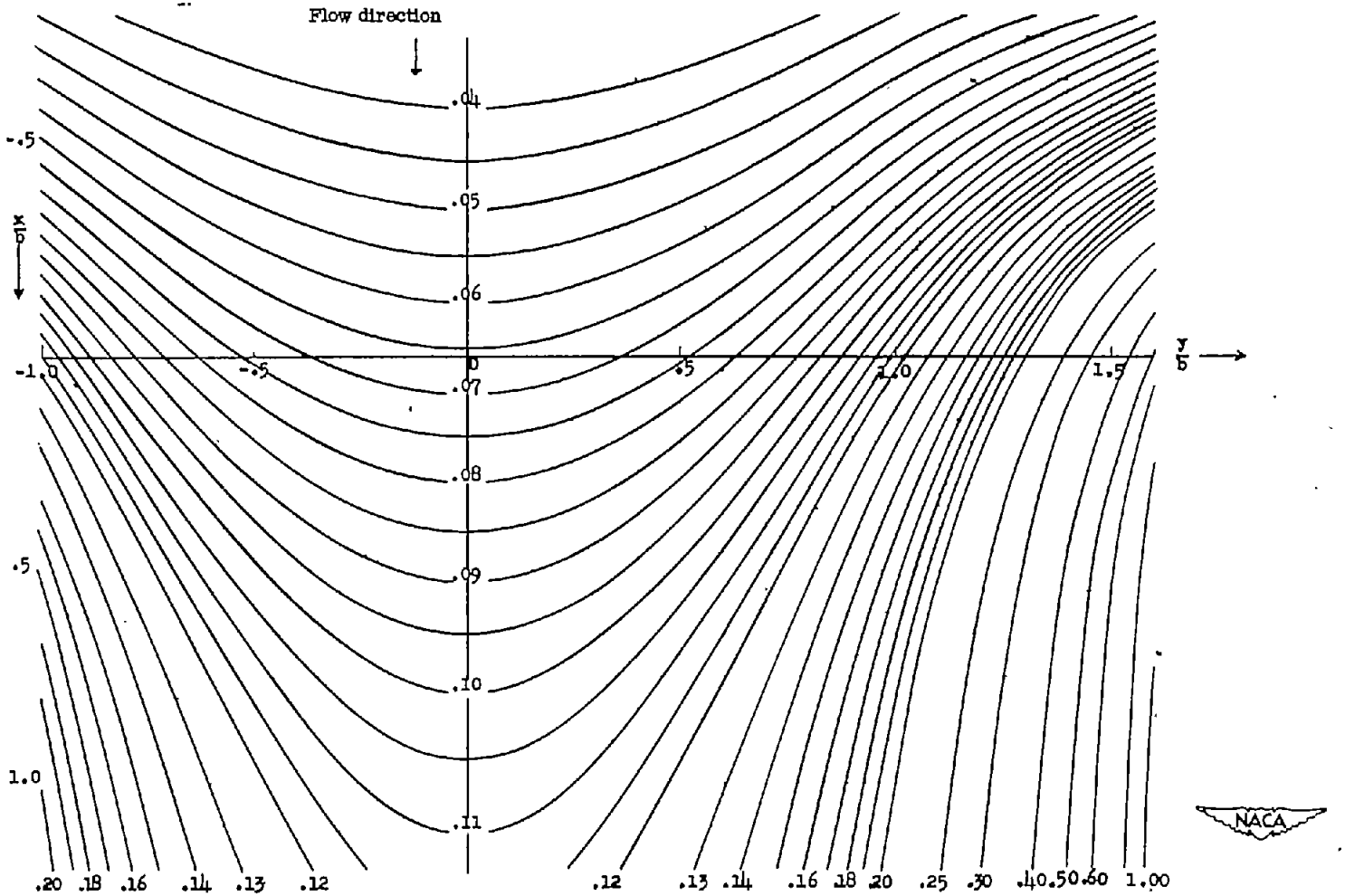

(b) Chart for Langley two-dimensional tunnels (3 by 7.5 ft); calculated for a 2 (horizontal) by 2.5 (vertical) array. The doublets alternate in sign vertically, with those in the horizontal center plane positive.

Figure 7.- Continued.

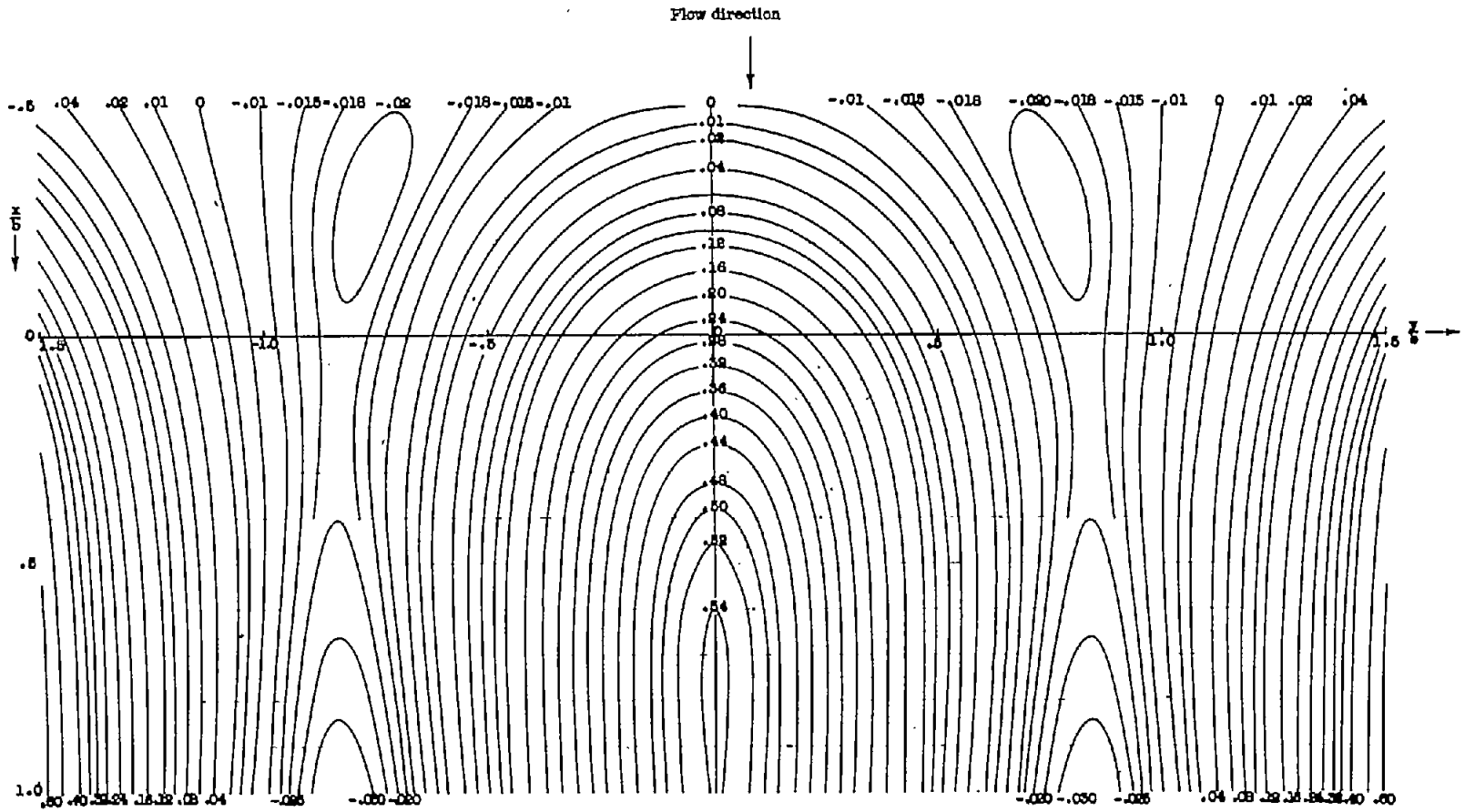

(c) Chart for 7- by 10-foot tunnels; calculated for a 2 (horizontal) by 0.7 (vertical) array. The doublets alternate in sign vertically, with those in the horizontal center plane positive.

Figure 7.- Concluded.

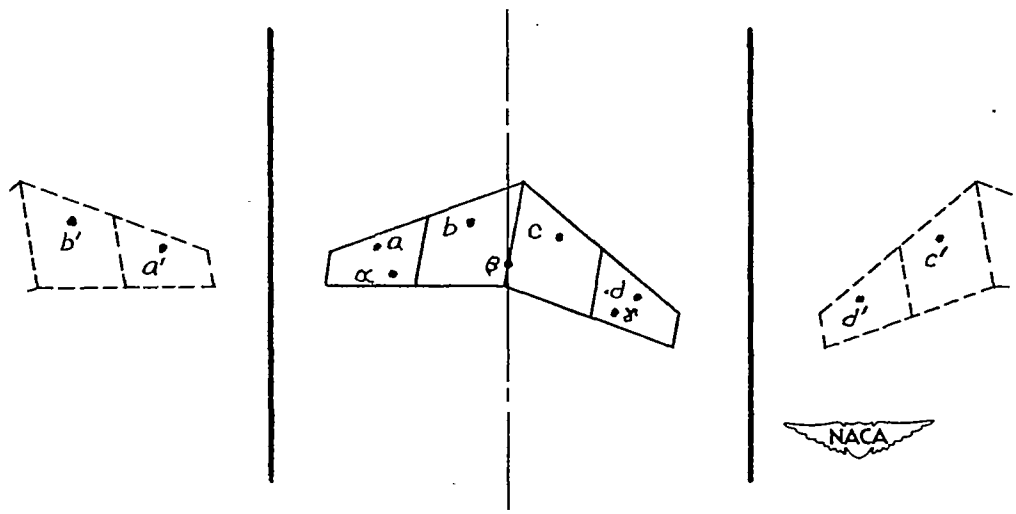

Figure 8.- Sketch used with charts A and B for determining tunnel-induced upwash angles. Sketch shows points a, b, c, and d where lift is assumed to be concentrated, the nearest images a', b', c', and d', and points α, β, and γ where the tunnel-induced upwash angles are to be determined.

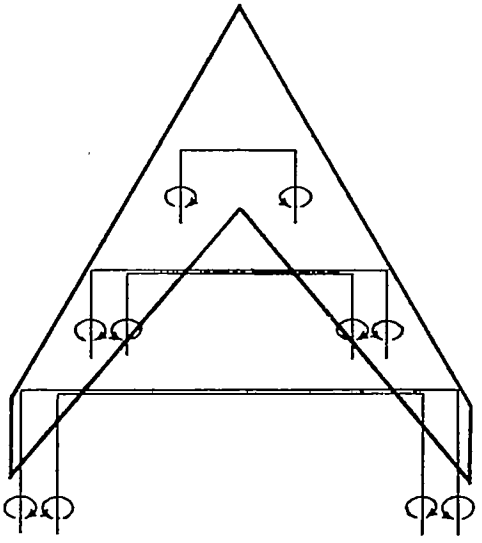

(a) Approximation by horseshoe vortices of 0° sweep.

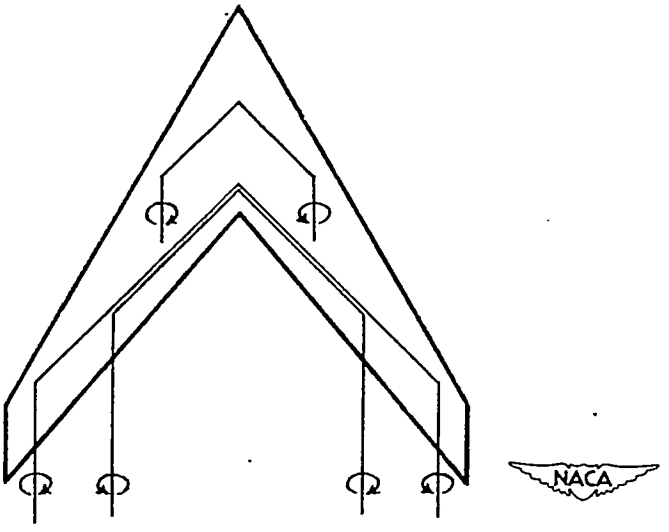

(b) Approximation by horseshoe vortices of 45° sweep.

Figure 9.- Approximation of the loading on a 60° sweptback wing by means of horseshoe vortices of different sweep.